



# Vesicle paleobarometry in the Pongola Supergroup: A cautionary note and guidelines for future studies

## **E.A. Goosmann**

Department of Earth and Space Sciences and Astrobiology Program, University of Washington, Seattle  
WA 98195-1310, USA  
e-mail: goosmann@uw.edu

## **R. Buick and D.C. Catling**

Department of Earth and Space Sciences and Astrobiology Program, University of Washington, Seattle  
WA 98195-1310, USA  
NASA Astrobiology Institute Virtual Planetary Laboratory, University of Washington, Seattle WA 98195-1580, USA  
e-mail: buick@uw.edu; dcatling@uw.edu

## **C. Luskin**

Department of Geology, University of Johannesburg, Johannesburg, South Africa  
e-mail: caseyl@uj.ac.za

## **N. Nhleko**

Geological Survey and Mines Department, Mbabane, Swaziland  
e-mail: nhlekon@swazi.net

© 2020 Geological Society of South Africa. All rights reserved.

## **Abstract**

Earth's global barometric pressure, currently 1 bar at sea level, may have changed over its 4.5-billion-year history. Proxy measurements, including  $N_2/^{36}Ar$  ratios in ~3.5 to 3.0 Ga hydrothermal quartz, ~2.7 Ga raindrop imprints, and ~2.7 Ga vesicle sizes in subaerial basalt lava flows indicate Archean air pressure could have been between 0.1 and 1.2 bar. However, some models argue air pressure in the Archean should have been much higher than now and could allow pressure broadening of greenhouse gas absorption lines to counteract the "Faint Young Sun". Thus, additional paleobarometric measurements would be useful to further constrain Earth's atmospheric evolution. We attempted to use vesicle sizes in lavas erupted near sea-level from the ~2.9 Ga Pongola Supergroup from Mahlangatsha and Mooihoek, eSwatini (formerly Swaziland) and the White Mfolozi River gorge of KwaZulu-Natal, South Africa to provide further Archean paleobarometric data. However, reliable results were unobtainable due to small and scarce amygdalae, irregular vesicle morphologies and metamorphic mineralogical homogenization preventing the use of X-ray Computed Tomography for accurate vesicle size determination. Researchers attempting paleobarometric analysis using lava vesicle sizes should henceforth avoid these areas of the Pongola Supergroup and instead look at other subaerially emplaced lava flows. With this being only the second time this method has been used on Precambrian rocks, we provide a list of guidelines informed by this study to aid future attempts at vesicular paleobarometry.

## Introduction

Earth's current sea level air pressure of 1 bar may have varied over geologic time because of changing partial pressures of nitrogen and other gases (Som et al., 2016; Stüeken et al., 2016a, 2016b). If so, this would have affected the height and magnitude of thermal boundaries in the lower atmosphere, in turn potentially influencing the vertical distribution of clouds, greenhouse gases, and redox species (Zahnle and Buick, 2016). However, there are very few geologic proxies that reliably record ancient air pressure. Raindrop imprints from ~2.7 Ga sedimentary rocks (Som et al., 2012) and the relationship of  $N_2/^{36}Ar$  to  $N_2/^{40}Ar$  from fluid inclusions trapped in quartz at ~3.5 to 3.0 Ga (Marty et al., 2013) and ~3.3 Ga (Avicé et al., 2018) combine to constrain the Archean air pressure upper limit to <1.2 bar ( $2\sigma$ ). Som et al. (2016) also addressed this question using the sizes of gas bubbles (vesicles when open, amygdales when mineralized) in ~2.7 Ga basaltic lava flows emplaced at sea level in the Boongal Formation, Rocklea Dome, Pilbara Craton, calculating an absolute air pressure within the range of >0 to 0.5 bar ( $2\sigma$ ).

These recent results disagree with other proxy interpretations, mantle geochemistry studies, and biogeochemical models. For instance, an alternative interpretation of the ~3.5 to 3.0 Ga fluid inclusions by Nishizawa et al. (2007) yielded a pressure of 3.3 bar, not <1.2 bar. Gradual atmospheric drawdown as a result of subduction sequestration of sedimentary nitrogen into the upper mantle has been suggested by numerous authors (e.g. Elkins et al., 2006; Li et al., 2007; Mitchell et al., 2010; Halama et al., 2014). Additionally, some models of nitrogen abundances in evolving terrestrial reservoirs argue that air pressure has monotonically decreased over time from Archean levels of ~2 bar (Goldblatt et al., 2009; Johnson and Goldblatt, 2015; Barry and Hilton, 2016; Mallik et al., 2018). Higher air pressure would have enhanced pressure broadening of greenhouse gas absorption lines, potentially helping to resolve the “Faint Young Sun” paradox (Sagan and Mullen, 1972).

However, monotonic nitrogen drawdown is not the only model for atmospheric pressure change through time. Som et al. (2016) suggested that atmospheric drawdown was restricted to the Archean, arguing that the two modern processes recycling nitrogen back to the atmosphere—oxidative weathering of organic material to nitrate ( $NO_3^-$ ) and subsequent denitrification to di-nitrogen gas ( $N_2$ )—were inoperative under the oxygen-free Archean atmosphere. In the mostly anoxic ocean, ammonium ( $NH_4^+$ ), would have been the generally stable form of nitrogen, not  $NO_3^-$ . Consequently, biological fixation, organic burial, and subduction of  $NH_4^+$  bound into potassic clays would have been possible due to the lack of the nitrification and denitrification pathways. This would have caused drawdown of atmospheric  $N_2$  between the advent of nitrogen fixation prior to ~3.2 Ga (Stüeken et al., 2015) and the Great Oxidation Event at ~2.3 Ga (Bekker et al., 2004). At the rise of oxygen, the rates of oxidative weathering, nitrification and denitrification would have increased significantly, reversing the drawdown trend and eventually raising atmospheric pressure to near-modern levels.

Complicating the picture further, a recent experimental study (Förster et al., 2019) of nitrogen partitioning during sediment subduction yielded contradictory outcomes for Archean atmospheric pressure depending on the rates of mantle degassing: lower if like modern, higher if much greater. So, given the large range in uncertainties in the paleobarometric data and the opposing model results, more quantitative constraints over a broader time range are needed for an accurate understanding of atmospheric evolution.

The paleobarometric method that yields the most quantitative results uses vesicle sizes in basaltic lava flows, as developed by Sahagian and colleagues. The idea that volume ratios between vesicles at the base and top of flows record changes in air pressure (e.g., Sahagian, 1985; Sahagian and Maus, 1994; Sahagian et al., 2002) relies on the combined gas law relationship, as expressed below by Som et al. (2016), between pressure ( $P$ ), temperature ( $T$ ), and volume ( $V$ ):

$$P_{air} = \rho g z \left( \frac{V_{top}}{V_{bot}} - 1 \right)^{-1} \quad (1)$$

Average vesicle volume at the top ( $V_{top}$ ) of a low-viscosity lava flow is relatively large and constrained by air pressure alone, while vesicles at the bottom ( $V_{bot}$ ) are smaller due to the combined air pressure and lithostatic pressure from the lava above it. Knowing the rock density ( $\rho$ ), the gravitational acceleration (for Earth  $g = 9.81 \text{ m/s}^2$ ), and flow thickness ( $z$ ), the size ratio between the basal and uppermost vesicles gives atmospheric pressure ( $P_{air}$ ). For an ancient basaltic lava flow to accurately record global air pressure at sea level, it must preserve all of the aforementioned measurable variables. Thus, a flow must show clear evidence for eruption close to sea level including: subaerial flow characteristics, stratigraphic proximity to sea level deposits, simple emplacement during a single lava pulse, and minimal post-depositional deformation (Sahagian et al., 2002).

A likely target for paleobarometric measurements using this method is the ~2.9 Ga Pongola Supergroup of southern Africa due to its well-preserved subaerial lavas (Wilson and Grant, 2006). Here, we examine the geological context of the Pongola Supergroup samples, discuss the factors that make the Pongola Supergroup of limited value for paleobarometry using the Sahagian et al. (2002) method, and provide some key observations for future field investigations looking to conduct vesicle paleobarometry using metamorphosed Precambrian lava flows.

## Geologic background

The Pongola Supergroup (Figure 1) is a well-preserved volcano-sedimentary succession (e.g. Armstrong et al., 1982, 1986; Wilson et al., 2013) deposited on the eastern margin of the Kaapvaal Craton in southern Africa at ~2.9 Ga (Hegner et al., 1994; Walraven and Pape, 1994; Mukasa et al., 2013; Gumsley

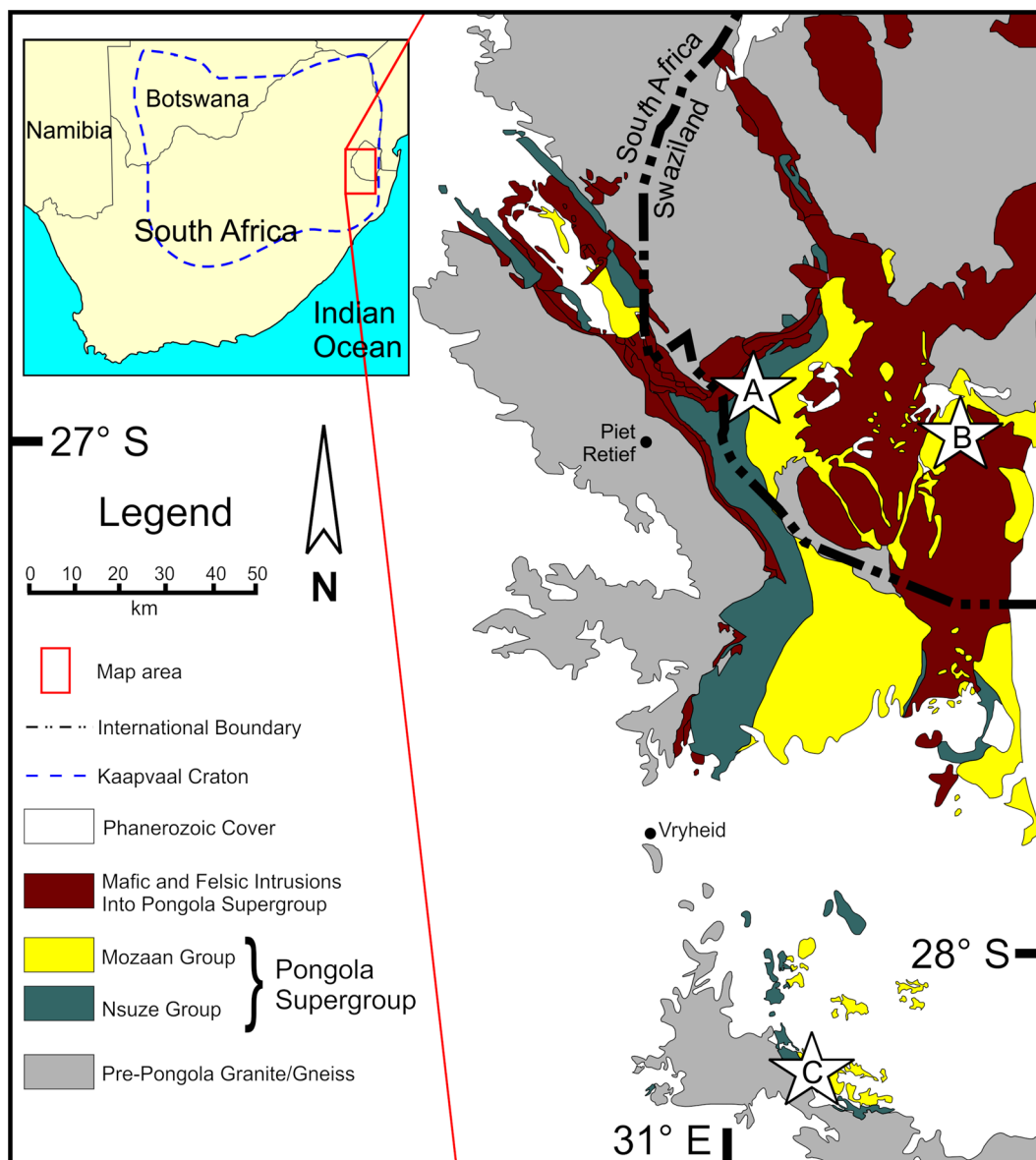


**Figure 1.** Geological map of the Pongola Supergroup in South Africa and eSwatini. Stars represent localities sampled in this study. Star A: Agatha Formation in the Mablangatsha area in eSwatini ( $S26.88995^{\circ}$ ,  $E031.02634^{\circ}$ ). Star B: Tobolsk Formation in the Mooihoek area in eSwatini ( $S26.98411^{\circ}$ ,  $E031.45418^{\circ}$ ). Star C: Agatha Formation in the White Mfolozi River gorge in South Africa ( $S28.23537^{\circ}$ ,  $E031.17999^{\circ}$ ). After Gold (2006), Wilson et al. (2013), Wilson and Hofmann (2013), and Gumsley et al. (2015).

et al., 2015). It is subdivided into two groups, shown in Figure 2. The lower Nsuze Group (Figure 2, left) is dominantly volcanic with interspersed sedimentary formations, whereas the upper Mozaan Group is dominantly sedimentary with minor volcanics (Figure 2, right). The Mozaan lies conformably above the Nsuze Group. Detailed descriptions and geochemistry of the sampled volcanic rocks can be found in Nhleko (2003) for the Pongola Supergroup in eSwatini (formerly Swaziland) and in Wilson and Grant (2006) for the Pongola Supergroup in South Africa. Wilson and Hofmann (2013) and Wilson et al. (2013) provide excellent overall summaries. Both the Tobolsk and Agatha formations within the Pongola Supergroup contain subaerial basalts and basaltic andesites potentially suitable for barometric analysis.

All rocks have been metamorphosed to lower-greenschist facies and vesicles have been infilled with secondary chlorite, calcite, and quartz to form amygdaloids.

In eSwatini, we sampled one flow from the Agatha Formation in the Mablangatsha area ( $S26.88995^{\circ}$ ,  $E031.02634^{\circ}$ ) and one flow from the Tobolsk Formation in the Mooihoek area ( $S26.98411^{\circ}$ ,  $E031.45418^{\circ}$ ) (Figure 1, localities A and B). In South Africa, we sampled 11 flows from the Agatha Formation in the White Mfolozi River gorge ( $S28.23537^{\circ}$ ,  $E031.17999^{\circ}$ ) (Figure 1, locality C).

For basalt flows to potentially record secular changes in air pressure, they must be emplaced near sea level under subaerial conditions, but not so high in elevation that air pressure is

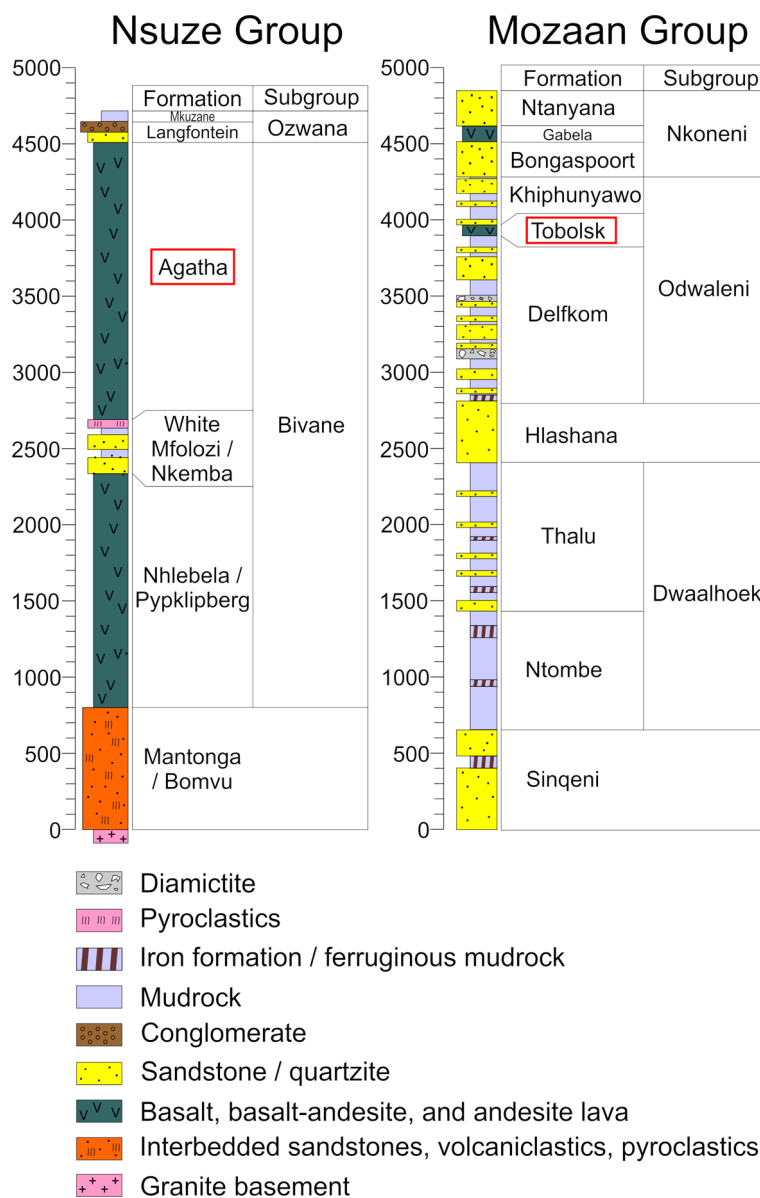


**Figure 2.** Generalized stratigraphic column of the Pongola Supergroup in South Africa and eSwatini. The Nsuzze Group (left) is dominantly volcanic with interspersed siliciclastic sediments, and the Mozaan Group (right) is dominantly siliciclastic with minor volcanics. The Mozaan lies conformably atop the Nsuzze Group, which is visible in the White Mfolozi River gorge (Figure 1 star C). The formation names surrounded by red boxes, Agatha and Tobolsk, are those that were sampled in this study. After Gold (2006), Wilson and Hofmann (2013) and Wilson et al. (2013).

significantly different. To confirm that the Pongola lava flows were emplaced close to sea level we looked for flow morphologies consistent with subaqueous deposition below sea level transitioning up to fully subaerial deposition. In all areas, the subaqueous to subaerial transition was evident, where basal pillowed flows with interstitial hyaloclastic breccia (Figure 3A) passed upwards into massive pāhoehoe flows with ropey tops, billowy surfaces and a total lack of pillows (Figure 3B). We sampled only those flows lying stratigraphically above the pillows but within 200 m of the transition. Other flow selection criteria included <3 m thickness, massive structure, simple emplacement (Figure 3C), preserved bottom and top chilled zones (Figure 3D), and few or no basal pipe amygdaloids

(Figure 3F) that might indicate secondary gas recharging, as advocated by Som et al. (2016).

## Methods

As was done by Som et al. (2016), the top and bottom ~10 cm of representative flows were sampled, cut with a diamond saw, examined in thin sections, and then analyzed using X-ray Computed Tomography (CT) following the methods described by Som et al. (2013). In short, X-rays passing through a rock are differentially attenuated by materials of differing density. CT records these changes in density and produces accurate internal 3D reconstructions of material changes without sample

destruction. We used an NSI X5000 scanning system with voltage of 140 kV and current of 180  $\mu$ A. The digitized CT reconstructions can then be used to measure vesicle/amygdale volumes and calculate air pressure using Equation 1.

## Results

The 0.31 m thick Tobolsk Formation flow (Figure 1 star B, Figure 4A) has ~1 mm diameter amygdales at the base comprising 1 to 2% of the rock. Amygdales increase to 1 to 3 mm diameter at the top comprising 5% of the rock. The amygdales are spherical, ellipsoidal, and irregular, showing evidence of vesicle amalgamation primarily in the middle vesicular zone but also at the top. The groundmass contains chlorite, plagioclase, actinolite, and titanite, and the amygdale infilling mineral is dominantly chlorite.

The 0.80 m thick Agatha Formation flow from eSwatini (Figure 1 star A, Figure 4B) has 1 to 2 mm diameter amygdales at the base comprising 4% of the rock. This transitions into a highly vesicular middle zone with coalesced amygdales reaching 1.5 cm diameter. The top (Figure 3D) contains 1 to 4 mm diameter amygdales, comprising ~8% of the rock. Figure 3E shows the transition from upper-middle to upper vesicular zone. Amygdales are rarely spherical and are typically ellipsoidal and irregular (Figure 3E and Figure 4B). The groundmass is chlorite, plagioclase, and titanite, and the amygdale infilling minerals are chlorite and calcite with microcrystalline quartz rims.

The 11 sampled flows of the Agatha Formation in South Africa (Figure 1 star C and Figure 4C) range from 0.26 to 2.75 m thick and all have similar vesicularity profiles. Bases contain  $\leq$ 1 mm diameter amygdales comprising 1 to 2% of the rock. Coalesced amygdales and numerous quartz-filled vugs 5 to

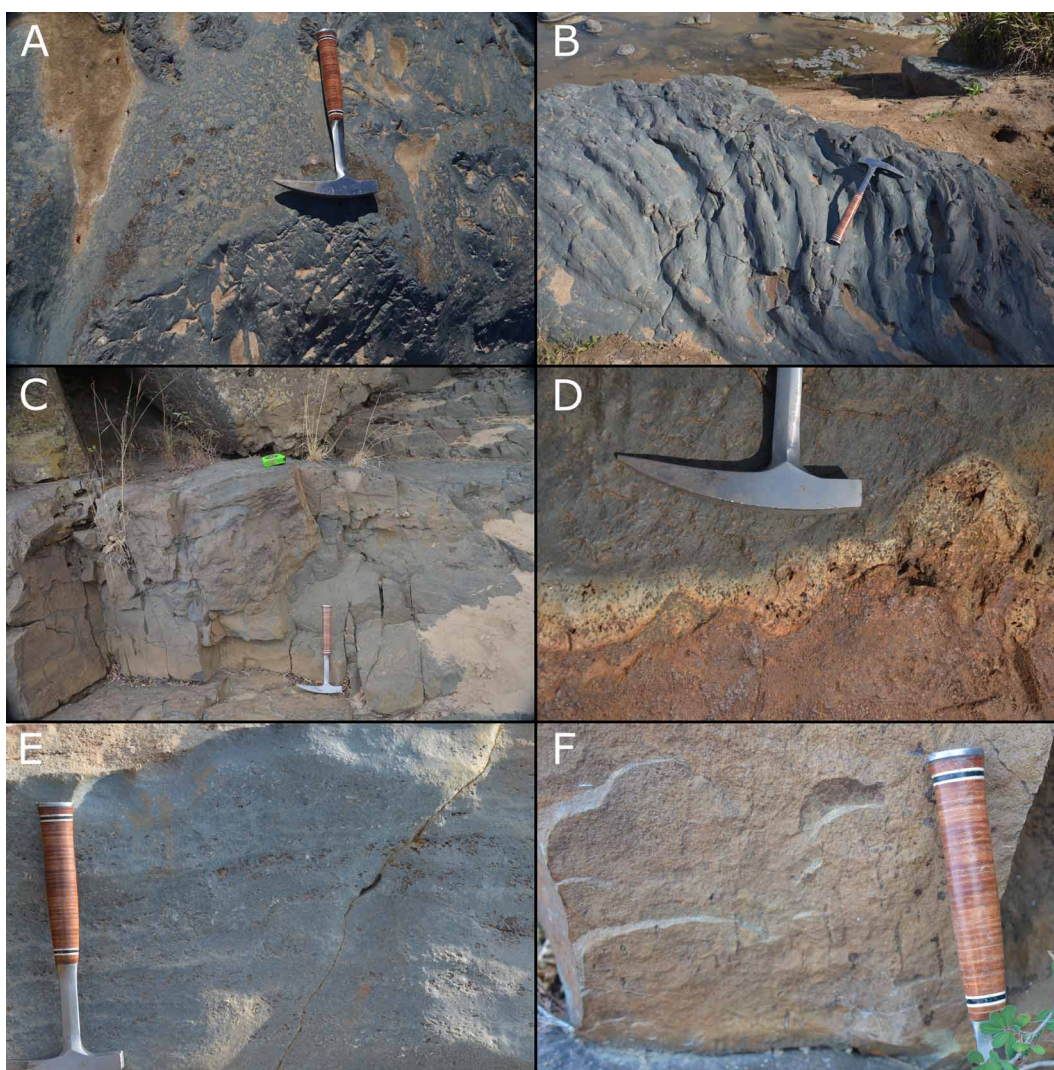


**Figure 3.** (A) Green, glassy interstitial hyaloclastic breccia (hammer handle) and dark grey pillow (hammer head). (B) Well-preserved ropey pāboeboe flow top. (C) Example of a massive, simply emplaced subaerial flow with billowy surface. (D) Example of a flow upper contact; yellow color is from weathering of glassy material. Amygdales in the chilled zone have been stretched. (E) Close-up of upper-middle and upper vesicular zone. Coalesced amygdales are visible along with spherical ones. (F) Example basal pipe vesicles. Hammer for scale in all images is 33 cm from head to handle. A to C and F from the Agatha Formation in South Africa, D to E from the Agatha Formation In eSwatini.

15 cm on the long-axis are visible within many flows. Flow tops have  $\leq 2$  mm diameter amygdaloids comprising up to 2 to 3% of the rock. Flows in the area that contained numerous basal pipe vesicles (e.g. Figure 3F) were avoided. The groundmass contains chlorite, calcite, plagioclase, titanite, and minor biotite. Amygdaloids are dominantly spherical and infilled with calcite with minor chlorite and biotite. The boundaries between the amygdaloids and groundmass are indistinct and can only be distinguished by the presence of calcite with smaller crystal sizes in the groundmass (Figure 4C).

In CT images, the Tobolsk Formation flow (Figure 5A) has amygdaloids easily distinguishable from the groundmass. The amygdaloids are irregularly shaped and often connected, similar to those seen in thin section (Figure 4A). The CT reconstruction of an Agatha Formation sample from South Africa (Figure 5B) confirms the amygdaloid sphericity observed in thin section (Figure 4C), but their small size and low density contrast with the groundmass makes them difficult to identify even with extreme contrast stretching in the images. For comparison, Figure 5C shows an example of a CT scan of a younger Fortescue Group sample from the Som et al. (2016) study. Compared to the Pongola Supergroup samples, it is much easier to identify amygdaloids and the amygdaloids are clearly spherical.

## Discussion

While many of the sampled flows did not have completely vesicle-free middle zones, they were clearly less vesicular than the basal and upper zones (e.g. Figure 3E). This still follows the typical vesicularity profile for simply emplaced flows (Figure 1 in Sahagian et al., 2002). In our flows, the amygdaloids in the middle vesicular zone were typically isolated amalgamated vesicles and vugs, which are features that typically result from coalescence, a common occurrence and cause of bimodal vesicle sizes in basalts (Sahagian et al., 2007). Thus these features are probably not evidence of a missing middle zone resulting from flow deflation. Instead, any vesicles in the middle zones are most likely a product of the flows being relatively thin, because central zones in flows thicker than  $\sim 3$  m are typically free of vesicles (Sahagian et al., 2002). However, we excluded such thick flows and only sampled flows  $< 2.75$  m to help avoid those that had undergone inflation. As a result, even with non-ideal vesicularity profiles, the Pongola samples were still suitable for the method and thus were scanned using CT.

Object size, mineral fill, and boundary sharpness all affect the utility of CT for analyzing geological samples. Small density differences and diffuse boundaries require extreme image contrast which introduces background noise effects. In the case of the Agatha Formation at the White Mfolozi River gorge in South Africa, the background noise effects can produce voxel (i.e. the three-dimensional equivalent of a pixel) sizes similar to those of some of the amygdaloids. This becomes problematic because any automated amygdaloid identification technique (e.g., Som et al., 2013) which can identify clearly defined spherical amygdaloids (Figure 5C) will produce just as many false positives as correct identifications. Though amygdaloids can instead be visually identified, the low vesicularity of the Pongola lava would

require inspection of at least 1200 CT image slices per sample to measure a statistically robust number of vesicle volumes. Som et al. (2016) measured as few as 236 vesicles in one of their flow bottoms, which resulted in a large  $2\sigma$  error in their final pressure calculation. While simply a guideline, 1 000 or more vesicle volumes at each flow top and bottom would reduce statistical error and should be the target number of measured vesicles. Moreover, amygdaloids comprised just 1 to 2% of the flow bottoms of the Agatha Formation in the White Mfolozi River gorge, increasing the number of visual inspections that would be required. Thus, the low vesicularity of flow bottoms are the chief limitation for visual amygdaloid identification. Overall, this makes CT impractical for vesicle paleobarometry of the Agatha Formation in the White Mfolozi River, South Africa.

The two eSwatini flows with the largest amygdaloids are the best targets for CT reconstruction considering the size and abundant problems noted for the South African site. However, from thin sections and CT scans it is evident that the amygdaloids in these flows are mostly irregular or ellipsoidal, presumably because their host rocks were originally basaltic andesites before metamorphism and not true basalts (Nhleko, 2003). In lavas more siliceous and thus more viscous than basalt, original vesicle morphologies will deviate from sphericity because of stretching along flow lines or because of incomplete air bubble fusion during amalgamation. These rocks thus provide a good case study as to why composition is important and why true basalts are the most useful for this method, which was calibrated using Hawaiian tholeiitic basalts on Mauna Loa (Sahagian et al., 2002) with a narrow range of  $\text{SiO}_2$  compositions from 47 to 52%. However, basalts and basaltic andesites effectively calculated uplift rates in the Central Anatolian Plateau in Turkey (Aydar et al., 2013) using a version of this method, indicating that some deviation from truly basaltic compositions can be accommodated.

Original sphericity is essential for automated CT measurement because it facilitates correct algorithm-based boundary identification. It also allows correction back to original spherical dimensions where post-depositional deformation has produced ellipsoidal amygdaloids. This difficulty can be overcome by structural back-correction if deformation has been simple, but in cases with initially ellipsoidal or irregular amygdaloids, this correction cannot be made. Since the eSwatini amygdaloids are ellipsoidal, irregular, and/or interconnected, we cannot infer that the vesicles were originally spherical or that the measured flow dimensions represent the initial flow thickness at the time when the upper and lower vesicular zones were frozen in the flow (term  $z$  in Equation 1). Thus these sites are also unsuitable for vesicle paleobarometry.

Overall, these results show that the ability of the CT scanning method to identify amygdaloids is the key limiting factor in such studies. The main difficulty with using CT on dense geological samples is that spatial resolution and density contrast from X-ray attenuation are connected. Low energy X-rays can pick out smaller density contrasts and smaller amygdaloids but are limited by complete attenuation in thick and dense samples. Consequently, for materials of similar density, such as in lower-greenschist facies metabasalt ( $\sim 2650$  kg/m<sup>3</sup>) and

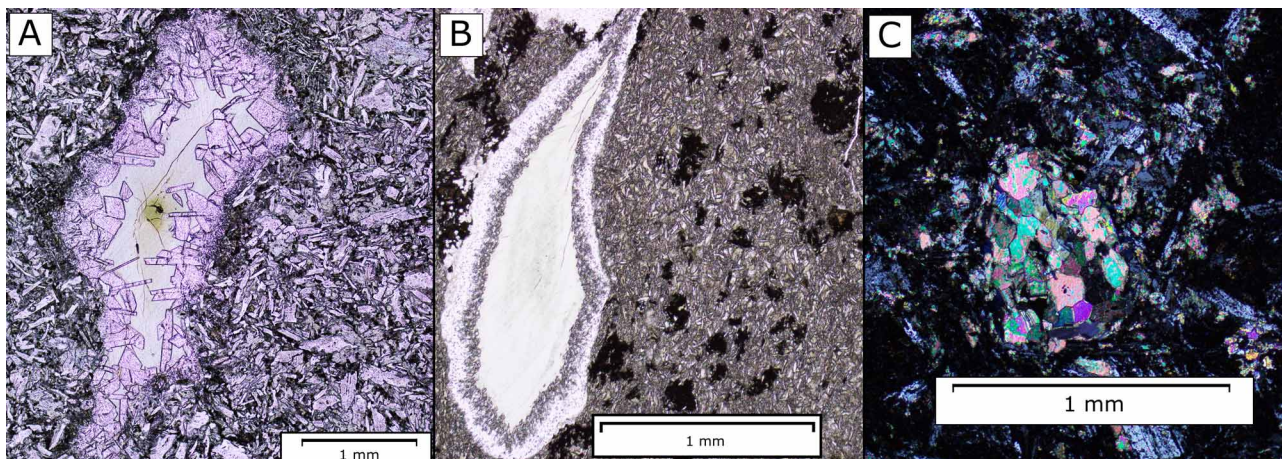


**Figure 4.** (A) Irregular chlorite-filled amygdale from the Tobolsk Formation in eSwatini in plane-polarized light. (B) Irregular chlorite-filled amygdale with a microcrystalline quartz reaction rim from the Agatba Formation in eSwatini in plane-polarized light. (C) Subspherical calcite and chlorite-filled amygdale from the Agatba Formation in South Africa. Image in cross-polarized light to highlight calcite. Note the calcite in the groundmass and diffuse boundary of the amygdale.

chlorite/calcite/quartz-filled amygdales ( $2650$  to  $2710$   $\text{kg/m}^3$ ), only larger amygdales can be reliably mapped (e.g., Figure 5C). Smaller amygdales with low density contrast can be identified if the distance from the scanner source is smaller and X-ray voltage is lower, but this requires that the samples are small and cut thinly, necessitating numerous scans of many sample cores to measure a statistically robust number of amygdales.

Other methods of amygdale measurement, such as serial sectioning, are possible but these destroy samples. Also, these techniques yield smaller amygdale diameters than the true diameters due to there being only one plane at which a spherical amygdale can be cut that would yield the true diameter. In the case of the Pongola lavas, the amygdales are on the order of 1 to 3 mm in diameter and the reduction in relative diameter on a given cross section would be a large

percentage of the total size of the amygdale. As such, visual measurements on cut rock faces, while possible in more vesicular lavas with cm-scale vesicles, could not be done for these Pongola samples.

#### Suggestions for future studies

Though this study did not yield meaningful paleopressure estimates, we combine our experiences with the results from Som et al. (2016), in addition to the original work by Sahagian, to formulate guidelines for future attempts. These guidelines expand upon the original method's selection criteria of subaerial emplacement, simple emplacement, basaltic composition, lack of secondary gas charge, and flow uniformity (Sahagian and Maus, 1994; Sahagian et al., 2002) by noting important

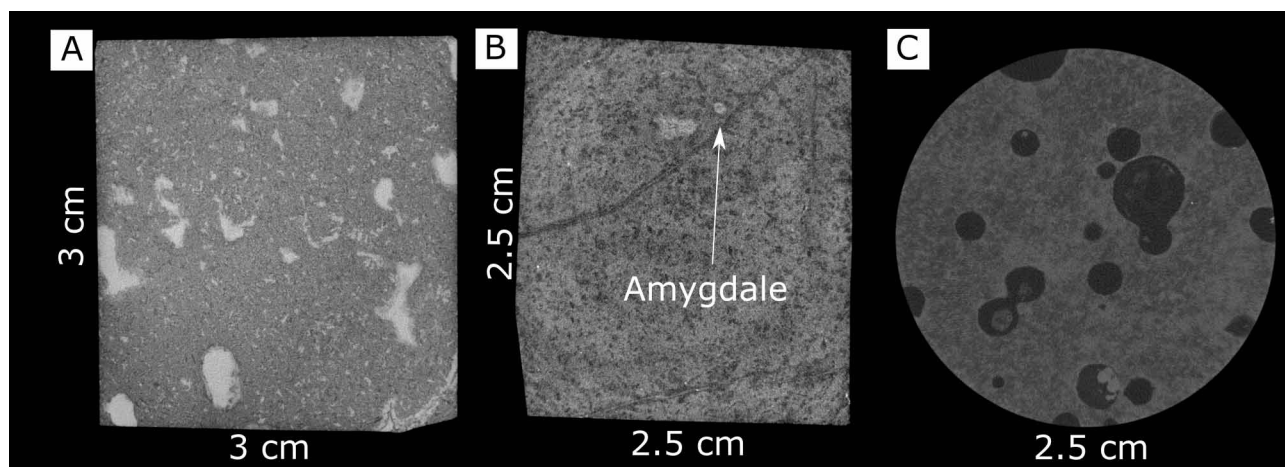


**Figure 5.** (A) Example of a CT image slice of the Tobolsk Formation in eSwatini, corresponding to Figure 4A. (B) Example of a representative CT image slice of the Agatba Formation in South Africa, corresponding to Figure 4C. (C) Example of a typical CT image slice taken of a Fortescue Group sample originally from Som et al. (2016) for comparison. Notice the sphericity of amygdales and the sharpness of their boundaries in C compared to A and B. In all images the higher density materials are brighter.

specifications for Precambrian rocks. Additionally, we provide new observation, sampling, and testing guidelines that should be noted when using this method on Precambrian flows.

*Subaerial emplacement:* This can be confirmed by the absence of subaqueous features, such as pillows, hyaloclastic breccia from quench fragmentation, interbedded chert or limestone, or peperite facies resulting from interaction with wet sediments, and the presence of pāhoehoe features such as ropey flow tops, hummocky flow surfaces or scoriaceous upper vesicular zones. In the absence of preserved pāhoehoe features, which aren't always evident in Precambrian rocks, traversing the transition from subaqueous features to the lack of subaqueous features, and/or observing interbedded pyroclastic material such as spatter, scoria, reticulite, and achneliths like Pele's tears and Pele's hair, all produced at subaerial basaltic vents, can support such an environmental interpretation.

*Solidification near sea level:* the flow should have subaqueous deposits within 100 stratigraphic meters from the sampled flow, otherwise any air pressure calculation could be a product of elevation difference. Features to identify such a setting include a subaqueous-to-subaerial transition with hyaloclastic breccia, pillow structures, interbedded chert and other subaqueous sediments, peperite facies, and pillow breccia underlying the massive flows.

*Mafic composition:* the flow must be basaltic. This method was calibrated on Hawaiian tholeiitic basalts, which have a narrow SiO<sub>2</sub> range. Basaltic flows have predictable vesicularity profiles that include: lower vesicular zones, middle vesicle-poor zones, and vesicle-rich upper vesicular zones (e.g. Sahagian, 1985; Sahagian and Proussevitch, 2007). Additionally, basaltic lavas have originally spherical vesicles, which can act as strain indicators. If a basalt flow's vesicles are non-spherical then post-depositional deformation has occurred, potentially altering flow thickness. Moreover, more siliceous lavas have more irregular vesicles that deviate from original sphericity towards more ellipsoidal or irregular. This could inhibit confirmation that the measured flow thickness is representative of the original flow thickness or the result of post-depositional deformation, which would require structural correction to determine air pressure from deformed vesicles. It also renders automated picking of amygdalae in CT scans problematic. However, it should be noted that this method has been used on basaltic andesites in the Central Anatolian Plateau in Turkey (Aydar et al., 2013).

*Simple emplacement:* the flow must result from a single lava pulse. Secondary lava addition (inflation), a common occurrence and a significant limitation for pāhoehoe lava flows, is indicated by non-standard vesicularity profiles with repeating vesicular zones or vesicle-rich middle zones. Vesicle cylinders (Goff, 1996), while less common, are also indicative of flow inflation (Fowler et al., 2015). Inflation produces a flow thicker than at the time when initial freezing established the uppermost and lowermost vesicle volumes, which would then produce erroneous pressure results and a middle zone that is highly

vesicular or has multiple vesicular zones within it. Lava loss (deflation) is indicated by missing middle vesicular zones or uniform vesicularity profiles. Deflation will distort the vesicularity profile of the flow and the measured flow thickness will be less than the actual thickness of the flow when vesicles at the top and bottom froze.

*Minimal post-depositional deformation:* the flow must preserve its original dimensions upon complete solidification. Any shortening or stretching will produce an apparent flow thickness that is not representative of the thickness when the vesicle volumes were frozen in. Additionally, later deformation can distort amygdale shape and may make it difficult to determine original sphericity. Most Precambrian terrains have undergone some deformation, so regions with minimal deformation are the best places to look for suitable flows.

*Modest and uniform thickness (0.3 to 3 meters):* the flow should be between 0.3 and 3 m thick consistently along strike. Flows <0.3 m may be products of deflation, introducing problems mentioned in guideline #4 (*Simple emplacement*). Additionally, in flows <0.3 m thick the vesicle size difference from the base to the top will be minimal due to the smaller pressure difference. Flows >3 m thick could be products of inflation and should be avoided due to the likely addition of gas during lava recharge (Sahagian et al., 2002). Additionally, thick flows could be the result of lava ponding, in which case they could degas before cooling enough to freeze in lower and upper vesicular zones.

*Absence of pipe vesicles:* the flow should have few or no pipe vesicles (e.g. Figure 3F) at its base. Pipe vesicles form by external addition of water vapor as the lava moves over a wet substrate, thus altering the initial gas charge of the flow. While a few pipe vesicles do not immediately exclude a flow from being used if it is sampled away from the pipes, abundant pipe vesicles can potentially change other vesicle volumes and profiles by addition of volatiles, producing an erroneous result (Sahagian and Proussevitch, 2007).

*Sufficient gas charge:* the flow should have sufficient vesicularity at the top and bottom for robust measurements. Higher vesicularity reduces the number of costly CT scans, makes amygdale identification using CT easier because the similar-density amygdalae appear more frequently and are thus more easily identified, resulting in overall larger vesicles that are more distinguishable when using CT. This usually occurs in pāhoehoe flows that are more proximal to the source vent and have degassed less than more distal 'a'ā flows. The flow base has a lower vesicularity than the top due to upward vesicle migration during flow emplacement, so paleobarometric measurement is functionally constrained by the basal vesicularity. We recommend a field measurement of at least 2 to 3% basal vesicularity for optimal sampling of a significant number of amygdalae.

*Smooth and regular contacts with underlying and overlying flows:* this precludes small-scale lithostatic pressure changes and

ensures even development of cooling fronts within the flow. This requirement effectively excludes 'a' flows and restricts paleobarometry to pāhoehoe flows without significant surface topography such as hornitos, tumuli etc.

*Specific sampling guidelines:* Samples of each flow for vesicle measurement should only include the upper and lower ~10 to 15 cm where the pressure difference is the greatest and is represented by the measured flow thickness for the pressure equation (Equation 1). If flows are vesicle-poor, more material should be sampled laterally across the flow rather than further inwards. When cored or cut for CT, avoid the uppermost and lowermost ~2 cm of flows where vesicles can be stretched by flow during initial freezing.

*General thin section analysis guidelines:* thin sections should be analyzed first to allow optimal sample selection for CT. While not fully quantitative, using known mineral density ranges and comparing amygdale mineral fill to the mineralogy of the groundmass can indicate which flows should be prioritized. Samples with greater mineralogical density contrast between matrix and amygdales have the greatest chance of analytical success. The samples should also have a  $\geq 5:1$  difference in crystal size between amygdale infill and rock matrix. If the matrix crystals are too large, it could introduce voxel noise into the CT scan and make amygdale identification more difficult. This ratio can be smaller if amygdales are large ( $>4$  mm) or amygdale infill has a significant density contrast with the matrix.

*CT analysis guidelines:* Samples should be cored into cylinders or cut into rectangular prisms (two sides with same dimension). This limits differential X-ray attenuation from thickness change as the sample rotates during scanning. Voltage, current, and distance from X-ray source will need to be individually adjusted for each flow based on sample properties (e.g. density, sample thickness). Moreover, due to differences in X-ray sources and detectors, each individual CT scanner will need to be calibrated to the samples. Spatial resolution (voxels/ $\mu\text{m}$ ), a product of the X-ray scanner voltage, current, and source distance, should be a small percentage of the mean amygdale size to ensure accurate diameter and volume measurements. Denser rocks require thinner sample cores or blocks to reach the same scan resolution due to attenuation of X-rays.

## Conclusion

The Pongola Supergroup in southern Africa contains well-preserved subaerial lavas that appear in outcrop to be suitable for vesicular paleobarometry. The Tobolsk Formation and Agatha Formation in eSwatini both have flows containing amygdales with clear boundaries that are visible in thin section and CT (Figures 4A, 4B and 5A), but their flow chemistry is more siliceous than tholeiitic basalt which created irregularly shaped amygdales, precluding them from being usable. The Agatha Formation in the White Mfolozi River in South Africa has numerous stacked flows of pāhoehoe basalt and the amygdales are mostly spherical in thin section (Figure 4C). However, the

very small size and low abundance of the amygdales due to low gas charge at solidification and the indistinct boundaries between chlorite/calcite amygdales and the chlorite/calcite groundmass means that CT is ineffective for identifying amygdales (Figure 5B). Moreover, this study indicates that although the Pongola Supergroup displays the correct depositional environment for vesicular paleobarometry and many primary features are well-preserved, primary composition, early degassing and post-depositional effects homogenizing mineralogy limit its utility for paleobarometric analysis. Other Precambrian subaerial basaltic lava flows emplaced at sea level (e.g. as listed in the supplemental materials in Kump and Barley (2007)) should instead be targeted for the calculation of ancient air pressure. Taking this as a learning experience, we include 12 guidelines for future vesicular paleobarometry studies using metamorphosed Precambrian lava flows.

## Acknowledgements

This work was supported by the NASA Astrobiology Institute's Virtual Planetary Laboratory Grant NNA13AA93A and a NASA Exobiology grant to RB (NNX16AI37G). We thank Allan Wilson and Ben Johnson for their critical and insightful reviews.

## References

- Armstrong, N., Hunter, D. and Wilson, A., 1982. Stratigraphy and petrology of the Archaean Nsuze Group, northern Natal and southeastern Transvaal, South Africa. *Precambrian Research*, 19, 75-107.
- Armstrong, N., Wilson, A. and Hunter, D., 1986. The Nsuze Group, Pongola Sequence, South Africa: geochemical evidence for Archaean volcanism in a continental setting. *Precambrian Research*, 34, 175-203.
- Avice, G., Marty, B., Burgess, R., Hofmann, A., Philippot, P., Zahnle, K. and Zakharov, D., 2018. Evolution of atmospheric xenon and other noble gases inferred from Archean to Paleoproterozoic rocks. *Geochimica et Cosmochimica Acta*, 232, 82-100.
- Aydar, E., Cubukcu, H.E., Erdal, Ş.E.N. and Lütfiye, A.K.I.N., 2013. Central Anatolian Plateau, Turkey: incision and paleoaltimetry recorded from volcanic rocks. *Turkish Journal of Earth Sciences*, 22, 739-746.
- Barry, P. and Hilton, D.R., 2016. Release of subducted sedimentary nitrogen throughout Earth's mantle. *Geochemical Perspectives Letters*, 2(2).
- Bekker, A., Holland, H.D., Wang, P.L., Rumble Iii, D., Stein, H.J., Hannah, J.L., Coetzee, L.L. and Beukes, N.J., 2004. Dating the rise of atmospheric oxygen. *Nature*, 427(6970), p117.
- Elkins, L.J., Fischer, T.P., Hilton, D.R., Sharp, Z.D., McKnight, S. and Walker, J., 2006. Tracing nitrogen in volcanic and geothermal volatiles from the Nicaraguan volcanic front. *Geochimica et Cosmochimica Acta*, 70, 5215-5235.
- Förster, M. W., Foley, S. F., Alard, O. and Buhre, S., 2019. Partitioning of nitrogen during melting and recycling in subduction zones and the evolution of atmospheric nitrogen. *Chemical Geology*, 525, 334-342.
- Fowler, A.C., Rust, A.C. and Vynnycky, M., 2015. The formation of vesicular cylinders in pahoehoe lava flows. *Geophysical and Astrophysical Fluid Dynamics*, 109, 39-61.
- Goff, F., 1996. Vesicle cylinders in vapor-differentiated basalt flows. *Journal of Volcanology and Geothermal Research*, 71, 167-185.
- Gold, D.J.C., 2006. The Pongola Supergroup. In: M.R. Johnson C.R. Anhaeusser and R.J. Thomas (Editors), *The Geology of South Africa*. Geological Society of South Africa / Council for Geoscience, Johannesburg / Pretoria, 135-147.
- Goldblatt, C., Claire, M.W., Lenton, T.M., Matthews, A.J., Watson, A.J. and

- Zahnle, K.J., 2009. Nitrogen-enhanced greenhouse warming on early Earth. *Nature Geoscience*, 2, 891-896.
- Gumsley, A., Olsson, J., Soderlund, U., de Kock, M., Hofmann, A. and Klausen, M., 2015. Precise U-Pb baddeleyite age dating of the Usushwana Complex, southern Africa – Implications for the Mesoarchean magmatic and sedimentological evolution of the Pongola Supergroup, Kaapvaal Craton. *Precambrian Research*, 267, 174-185.
- Halama, R., Bebout, G.E., John, T. and Scambelluri, M., 2014. Nitrogen recycling in subducted mantle rocks and implications for the global nitrogen cycle. *International Journal of Earth Sciences*, 103, 2081-2099.
- Hegner, E., Kröner, A. and Hunt, P., 1994. A precise U-Pb zircon age for the Archaean Pongola Supergroup volcanics in Swaziland. *Journal of African Earth Sciences*, 18, 339-341.
- Johnson, B. and Goldblatt, C., 2015. The nitrogen budget of Earth. *Earth-Science Reviews*, 148, 150-173.
- Kump, L.R. and Barley, M.E., 2007. Increased subaerial volcanism and the rise of atmospheric oxygen 2.5 billion years ago: *Nature*, v. 448, no. 7157, 1033p.
- Li, L., Bebout, G.E. and Idleman, B.D., 2007. Nitrogen concentration and  $\delta^{15}\text{N}$  of altered oceanic crust obtained on ODP Legs 129 and 185: Insights into alteration-related nitrogen enrichment and the nitrogen subduction budget. *Geochimica et Cosmochimica Acta*, 71, 2344-2360.
- Mallik, A., Li, Y. and Wiedenbeck, M., 2018. Nitrogen evolution within the Earth's atmosphere-mantle system assessed by recycling in subduction zones. *Earth and Planetary Science Letters*, 482, 556-566.
- Marty, B., Zimmermann, L., Pujol, M., Burgess, R. and Philippot, P., 2013. Nitrogen Isotopic Composition and Density of the Archean Atmosphere. *Science*, 342, 101-104.
- Mitchell, E.C., Fischer, T.P., Hilton, D.R., Hauri, E.H., Shaw, A.M., de Moor, J.M., Sharp, Z.D. and Kazahaya, K., 2010. Nitrogen sources and recycling at subduction zones: Insights from the Izu-Bonin-Mariana arc. *Geochemistry, Geophysics, Geosystems*, 11(2).
- Mukasa, S.B., Wilson, A.H. and Young, K.R., 2013. Geochronological constraints on the magmatic and tectonic development of the Pongola Supergroup (Central Region), South Africa. *Precambrian Research*, 224, 268-286.
- Nhleko, N., 2003. The Pongola Supergroup in Swaziland: PhD thesis, Rand Afrikaans University (now University of Johannesburg), 299pp.
- Nishizawa, M., Sano, Y., Ueno, Y. and Maruyama, S., 2007. Speciation and isotope ratios of nitrogen in fluid inclusions from seafloor hydrothermal deposits at 3.5 Ga. *Earth and Planetary Science Letters*, 254, 332-344.
- Sagan, C. and Mullen, G., 1972. Earth and Mars: Evolution of atmospheres and surface temperatures. *Science*, 177, 52-56.
- Sahagian, D., 1985. Bubble migration and coalescence during the solidification of basaltic lava flows. *The Journal of Geology*, 93, 205-211.
- Sahagian, D.L. and Maus, J.E., 1994. Basalt vesicularity as a measure of atmospheric pressure and palaeoelevation. *Nature*, 372, 449.
- Sahagian, D. and Proussevitch, A., 2007. Paleoelevation measurement on the basis of vesicular basalts. *Reviews in Mineralogy and Geochemistry*, 66, 195-213.
- Sahagian, D.L., Proussevitch, A.A. and Carlson, W.D., 2002. Analysis of vesicular basalts and lava emplacement processes for application as a paleobarometer/paleoaltimeter. *Journal of Geology*, 110, 671-685.
- Som, S.M., Catling, D.C., Harnmeijer, J.P., Polivka, P.M. and Buick, R., 2012. Air density 2.7 billion years ago limited to less than twice modern levels by fossil raindrop imprints. *Nature*, 484, 359-362.
- Som, S.M., Hagadorn, J.W., Thelen, W.A., Gillespie, A.R., Catling, D.C. and Buick, R., 2013. Quantitative discrimination between geological materials with variable density contrast by high resolution X-ray computed tomography: An example using amygdule size-distribution in ancient lava flows. *Computers and Geosciences*, 54, 231-238.
- Som, S.M., Buick, R., Hagadorn, J.W., Blake, T.S., Perreault, J.M., Harnmeijer, J.P. and Catling, D.C., 2016. Earth's air pressure 2.7 billion years ago constrained to less than half of modern levels. *Nature Geoscience*, 9, 448-451.
- Stüeken E.E., Buick R., Guy B.M. and Koehler M.C., 2015. Isotopic evidence for biological nitrogen fixation by molybdenum-nitrogenase from 3.2 Gyr. *Nature*, 520, 666-669.
- Stüeken, E., Kipp, M., Koehler, M., Schwieterman, E., Johnson, B. and Buick, R., 2016a. Modeling  $\text{pN}_2$  through geological time: Implications for planetary climates and atmospheric biosignatures. *Astrobiology*, 16, 949-963.
- Stüeken, E.E., Kipp, M.A., Koehler, M.C. and Buick, R., 2016b. The evolution of Earth's biogeochemical nitrogen cycle. *Earth-Science Reviews*, 160, 220-239.
- Wälraven, F. and Pape, J., 1994. Pb-Pb whole-rock ages for the Pongola supergroup and the Usushwana Complex, South Africa. *Journal of African Earth Sciences*, 18, 297-308.
- Wilson, A., Groenewald, B. and Palmer, C., 2013. Volcanic and volcanoclastic rocks of the Mesoarchean Pongola Supergroup in South Africa and Swaziland: distribution, physical characteristics, stratigraphy and correlations. *South African Journal of Geology*, 116, 119-168.
- Wilson, A.H. and Grant, C.E., 2006. Physical volcanology and compositions of the basaltic lavas in the Archean Nzuse Group, White Mfolozi inlier, South Africa. *Geological Society of America Special Papers*, 405, 255-289.
- Wilson, A.H. and Hofmann, A., 2013. The Meso-Archaean Pongola Supergroup in South Africa and Swaziland — The oldest known large igneous province on stable continental crust? Large Igneous Provinces Commission, June 2013 LIP of the Month.
- Zahnle, K. and Buick, R., 2016. Atmospheric science: Ancient air caught by shooting stars. *Nature*, 533, 184-186.

Editorial handling: M.A. Elburg.